Electronic Supplementary Material (ESI) for Journal of Materials Chemistry A.

Supplementary Information

Understanding the impact of Bi stoichiometry towards optimised $BiFeO_3$ photocathodes: structure, morphology, defects and ferroelectricity

Haozhen Yuan[1], Subhajit Pal[1], Chloe Forrester[1], Qinrong He[1] and Joe Briscoe[1*]

[1]*School of Engineering and Materials Science, Queen Mary University of London, London, E1 4NS, United Kingdom*

[*]*Corresponding author: j.briscoe@qmul.ac.uk*

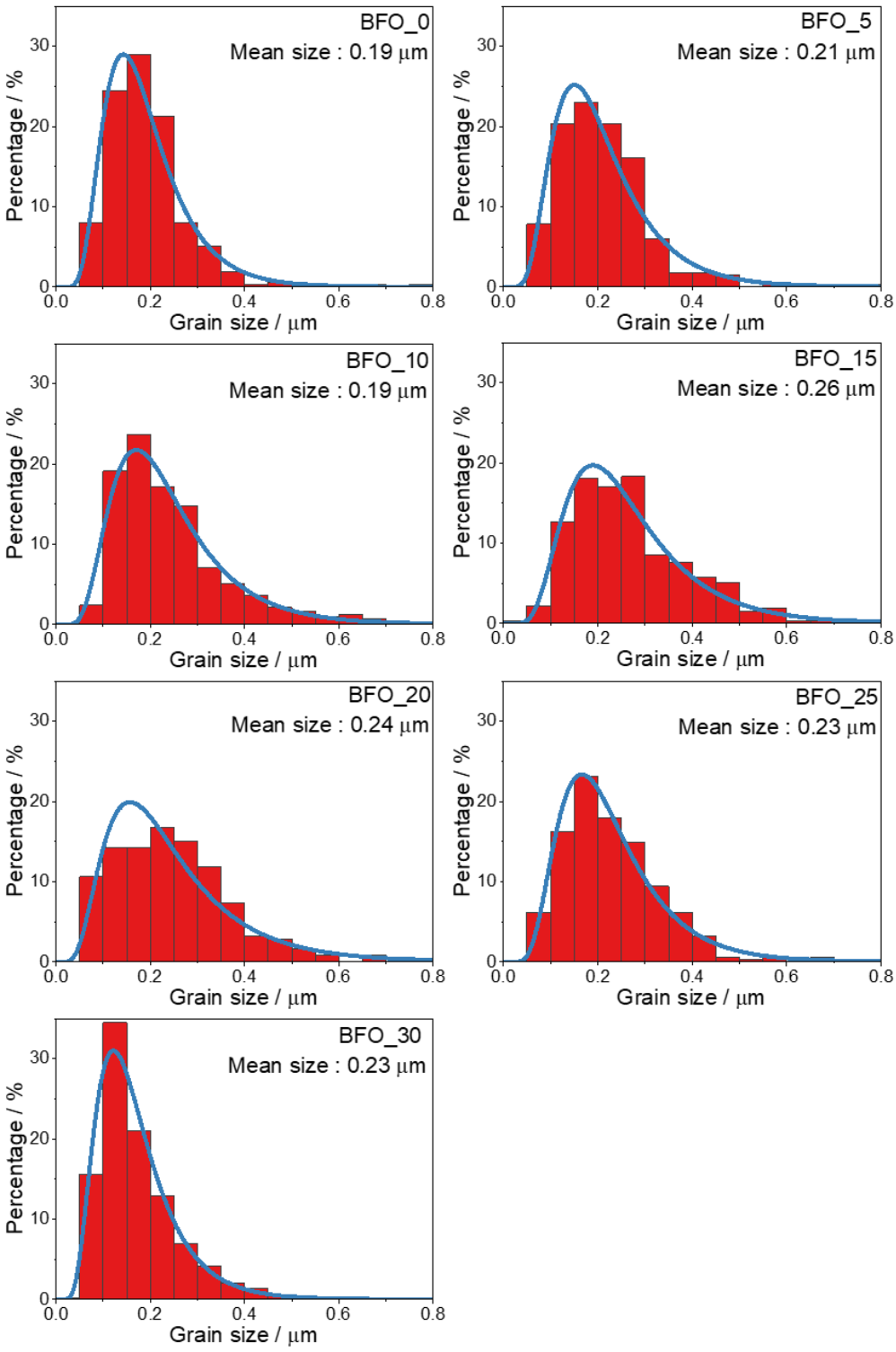

Figure S1 Grain size distribution of $Bi_{1+x}FeO_3$ films measured from SEM top-view images.

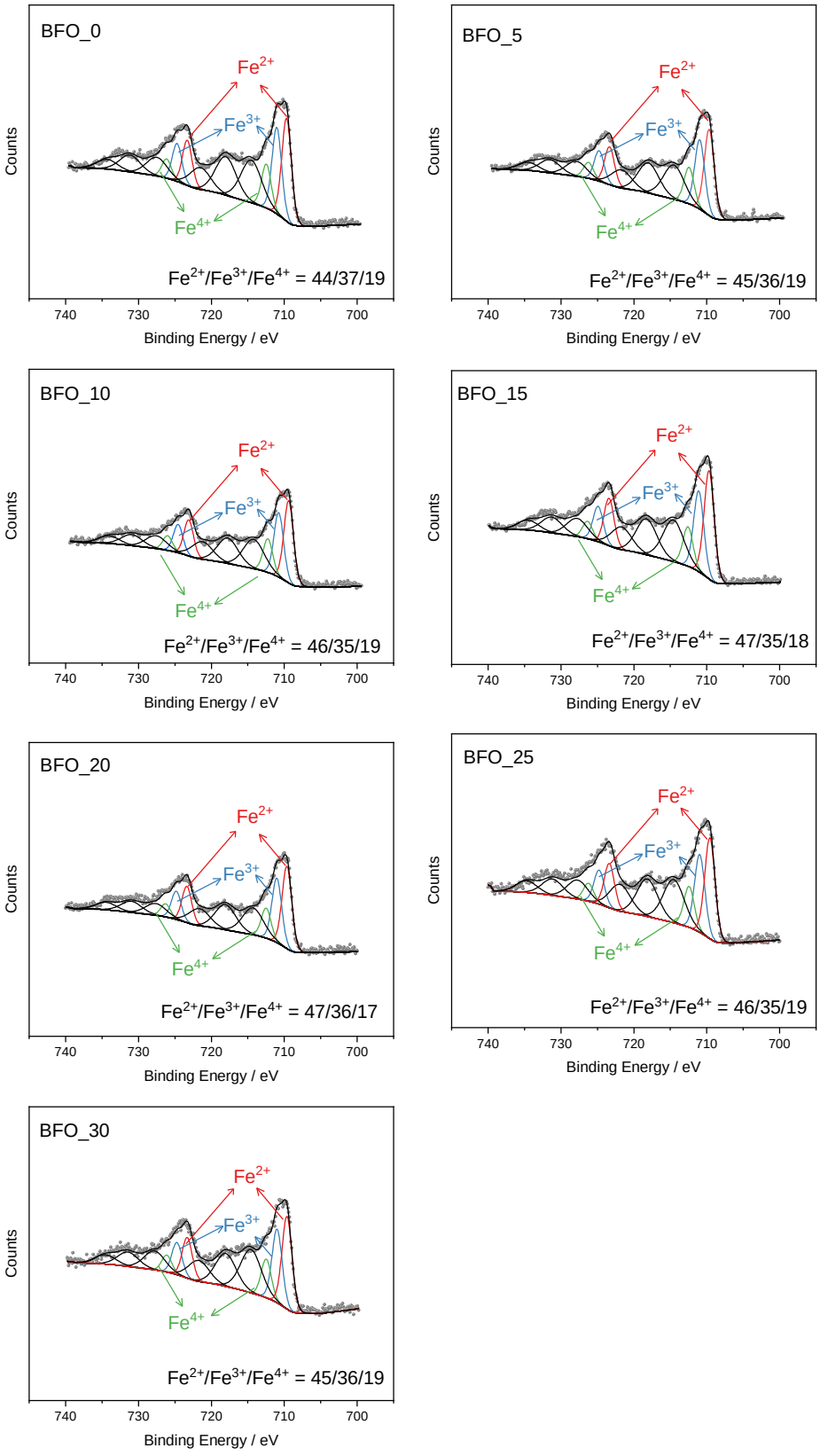

Figure S2 XPS Fe2p narrowed scan of $Bi_{1+x}FeO_3$ films, fitted with 3 main peaks of Fe^{2+}, Fe^{3+} and Fe^{4+} and associated satellite peaks.

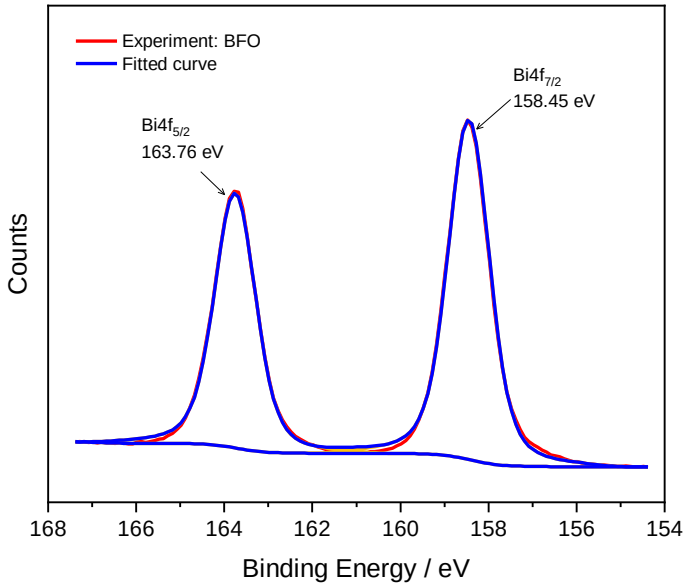

Figure S3 XPS Bi4f narrowed scan of $Bi_{1+x}FeO_3$ films.

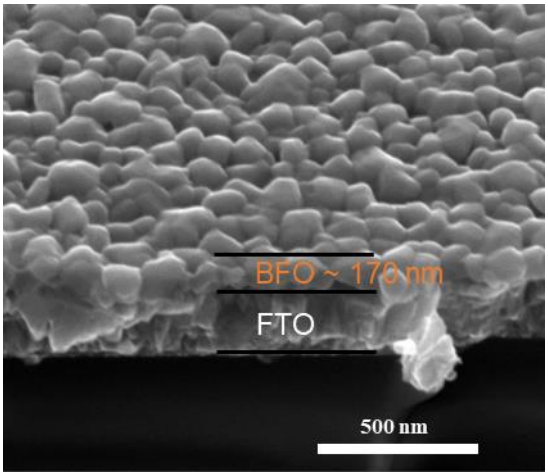

Figure S4 Cross-sectional SEM images which shows that BFO_10 film have a thickness of around 170 nm. Ten points were measured which give the mean thickness of 170.0 nm, the maximum thickness of 197.4 nm and the minimum thickness of 143.3 nm.

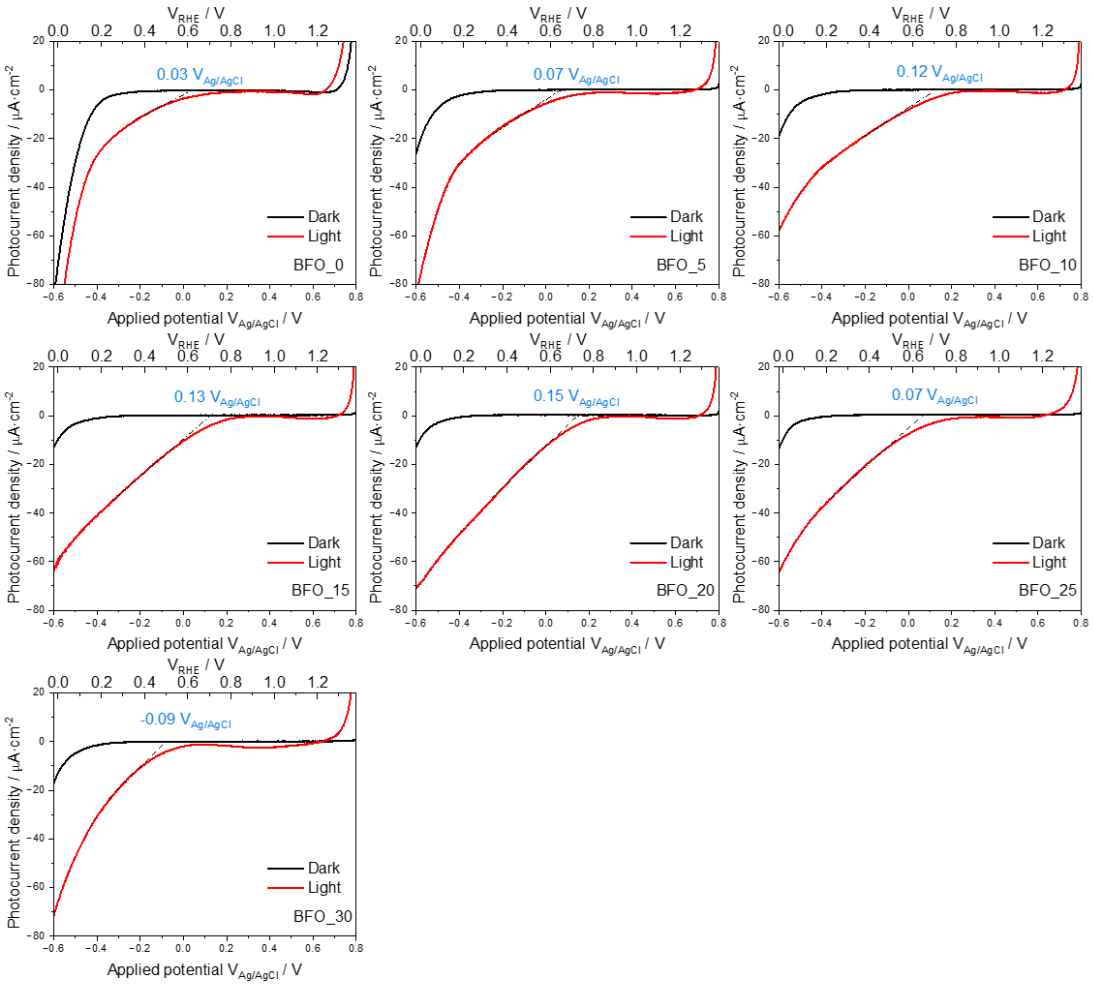

Figure S5 LSV measurements of $Bi_{1+x}FeO_3$ thin films under dark and 1.5G AM illumination in 0.2 M Na_2SO_4 electrolyte with onset potential presented.

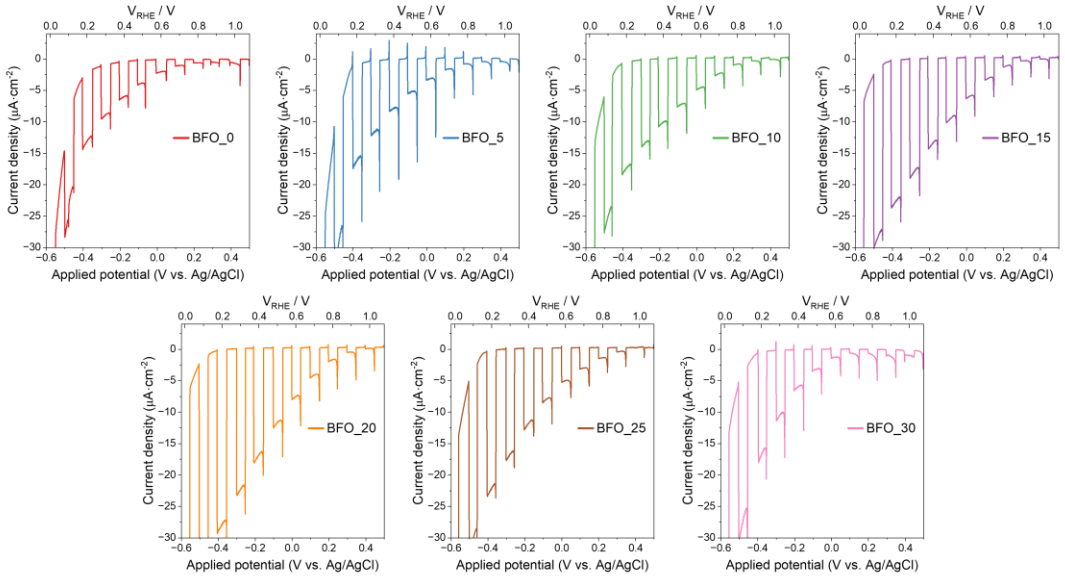

Figure S6 LSV measurements of all $Bi_{1+x}FeO_3$ thin films under chopped illumination in 0.2 M Na_2SO_4 electrolyte.

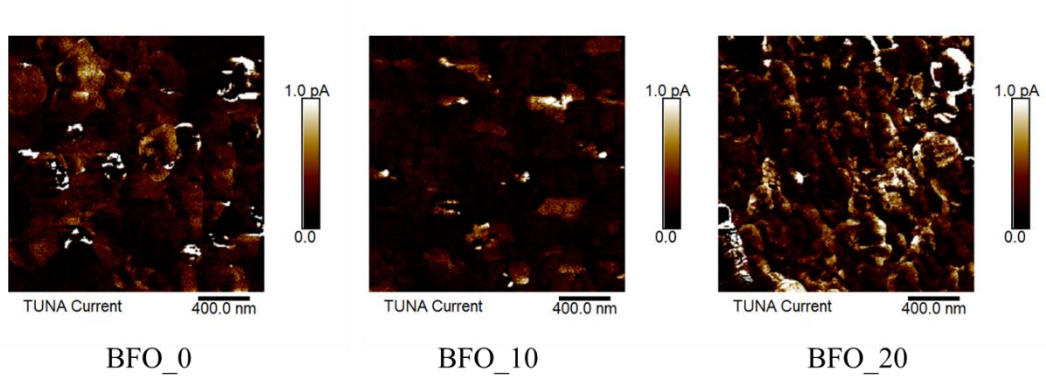

Figure S7 C-AFM photocurrent images of BFO_0, 10 and 20 by subtracting current images under dark from those under 391 nm illumination. A DC bias of -3V was applied at the tip.

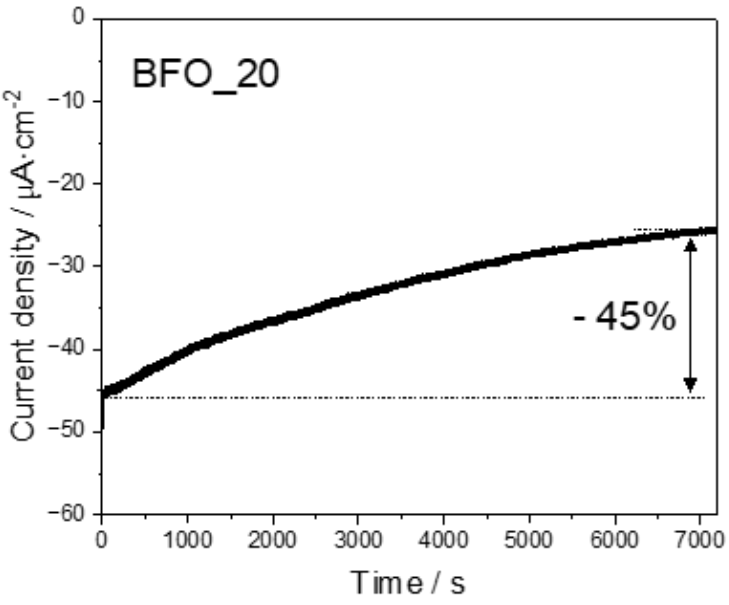

Figure S8 LSV curve of BFO_20 measured under illumination over 1 hour**.**

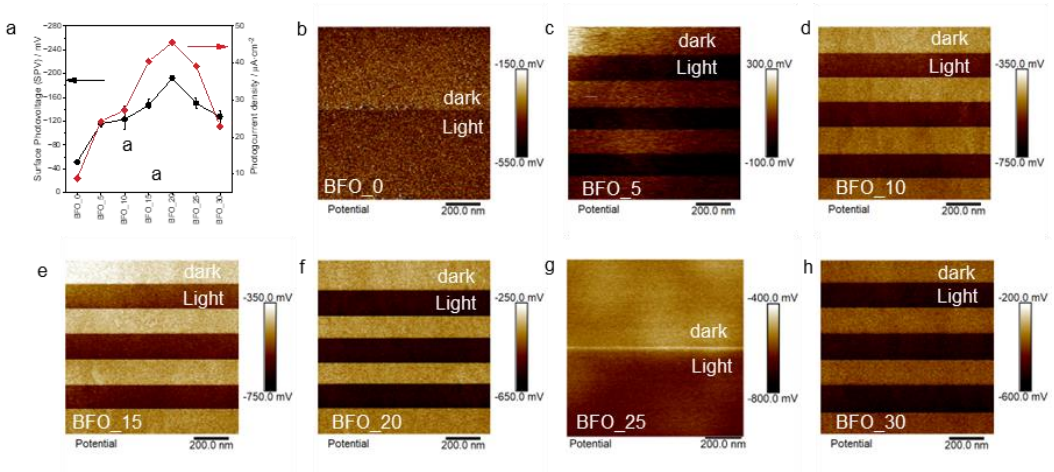

Figure S9 (a) Photocurrent density measured at 0.2 V vs. RHE (red line) and surface voltage (black line) calculated by the difference between CPD under dark and light illumination condition of $Bi_{1+x}FeO_3$ films. (b-h) KPFM measurements of $Bi_{1+x}FeO_3$ under dark and 391 nm illumination. The range of scale bars is fixed at 400 mV so that the contrast in different samples can be easily compared with each other. The SPV was measured by the difference of CPD between dark and light.

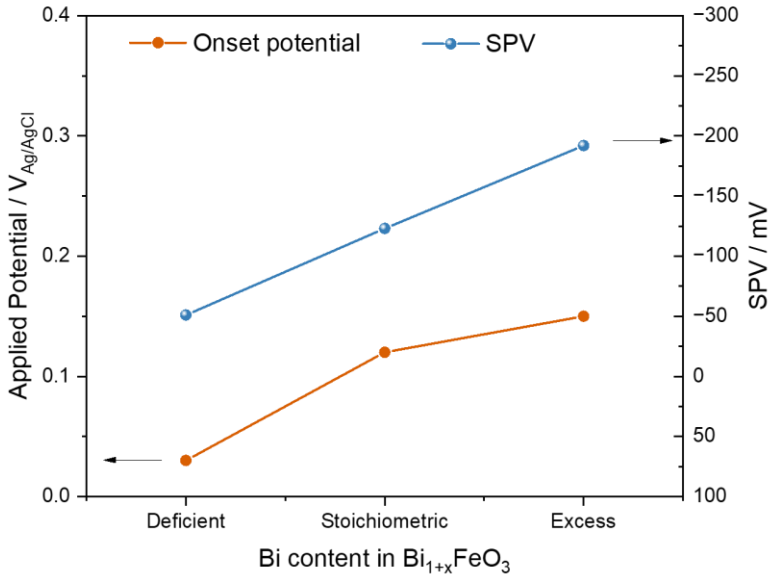

Figure S10 The relationship between onset potential and SPV results.

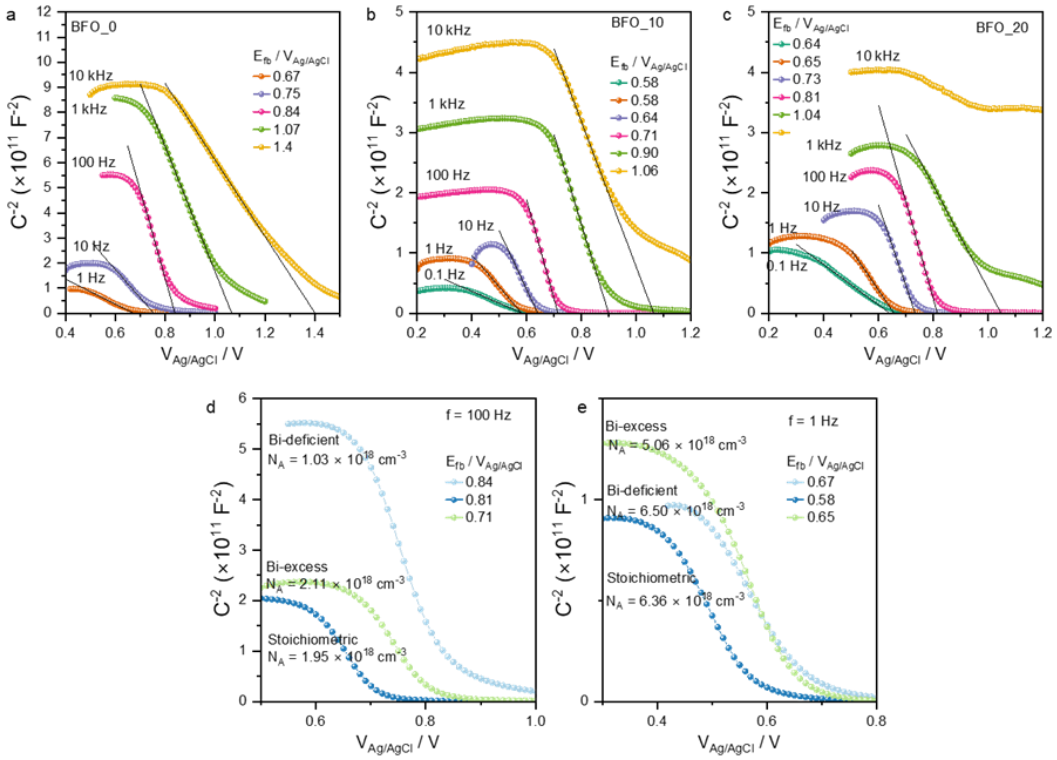

Figure S11 The Mott Schottky plots of (a) BFO_0 Bi-deficient BFO, (b) BFO_10 stoichiometric BFO and (c) BFO_20 Bi-excess BFO measured with different frequency from 1 Hz to 10 kHz. The comparison of Mott Schottky plots of these 3 films at 1 Hz (d) and 100 Hz (e).

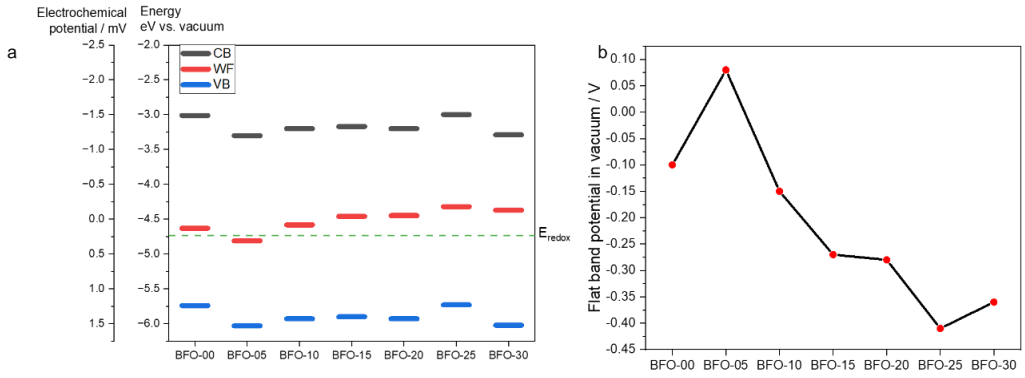

Figure S12 (a) Band diagram of $Bi_{1+x}FeO_3$ films. V_{CB}, V_F and V_{VB} represents the energy level of conduction band, Fermi level and valence band, respectively. The green dash lines represents the energy level of water reduction and oxidation half reaction at pH=6.5. (b) Estimated flat band potential in vacuum calculated from the band bending after equilibrium is reached between the Fermi level of the photoelectrode and the average redox potential of the electrolyte.

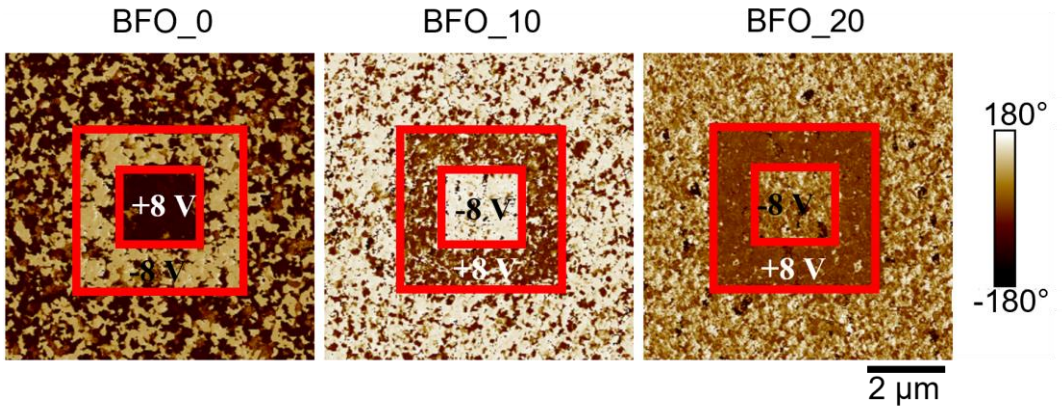

Figure S13 PFM phase images BFO_0, BFO_10 and BFO_20 thin film. Images were taken in 8 × 8 μm^2 after +/-8 V poling in the 4 × 4 and 2 × 2 μm^2 areas, respectively.

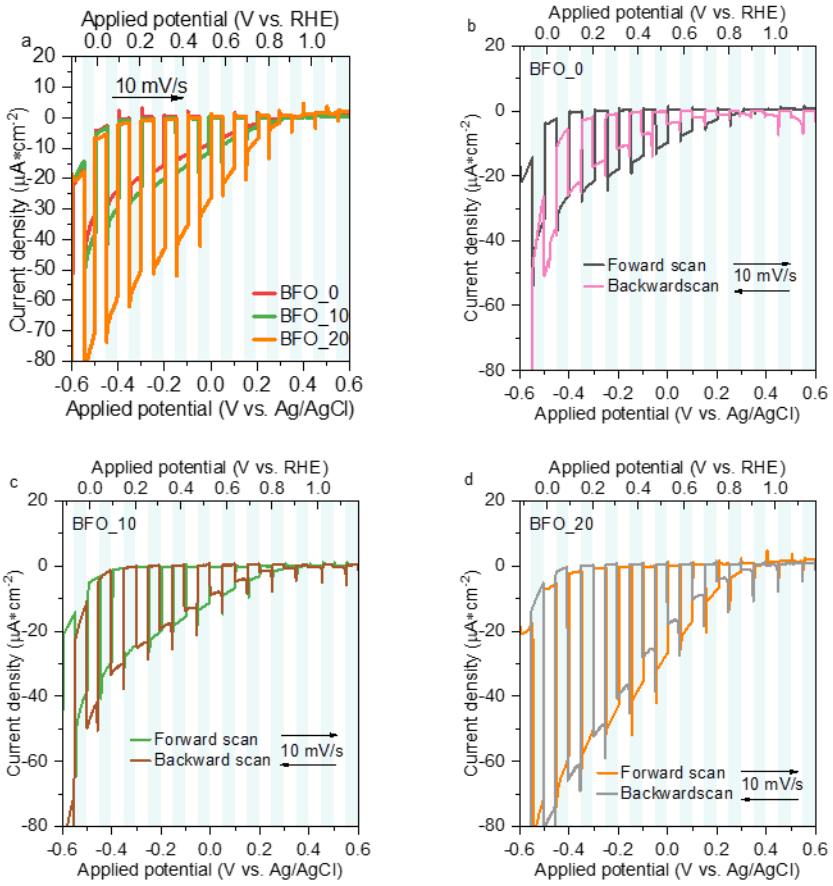

Figure S14 (a)LSV measurements of BFO_0, BFO_10 and BFO_20 thin films under chopped illumination in 0.2 M Na_2SO_4 electrolyte with the forward scanning direction from -0.6 to 0.6 V vs. Ag/AgCl; The comparison between forward (negative to positive potential) and backward (positive to negative potential) scan in BFO_0 (a), BFO_10 (b) and BFO_20 (c) films